Electronic structure of the (2×2)C $p4g$ carbidic phase on Ni{100}

C. F. McConville and D. P. Woodruff
Physics Department, University of Warwick, Coventry CV4 7AL, England, United Kingdom

S. D. Kevan*
AT&T Bell Laboratories, Murray Hill, New Jersey 07974-2070

M. Weinert and J. W. Davenport
Physics Department, Brookhaven National Laboratory, Upton, New York, 11973-5000
(Received 24 February 1986)

Angle-resolved photoemission measurements of the valence-electronic structure of the Ni{100}(2×2)C structure are compared with the results of self-consistent density-functional calculations of the two-dimensional band structure for a $c(2\times2)$C overlayer on Ni{100}. Good agreement is found for the energies of the main C $2p$– and C $2s$–related features at $\bar{\Gamma}$ and the computed dispersion is similar to, but somewhat greater than, that observed experimentally. These experimental features map in the $c(2\times2)$ surface Brillouin zone defined by the carbon overlayer, and not the (2×2) zone of the surface reconstruction. Changes in the d band structure are attributed to this reconstruction and are not found in the calculated bands or in experiments on a $c(2\times2)$O overlayer, both of which involve unreconstructed surfaces.

I. INTRODUCTION

In this paper we present the results of an investigation into the electronic structure of the Ni{100}(2×2)C surface using both angle-resolved ultraviolet photoelectron spectroscopy (ARUPS) and self-consistent calculations on slab structures using the density-functional formalism. This carbidic surface phase is known to be the steady state ("active") phase of the surface of a Ni{100} catalyst in the methanation reaction.[1] Indeed, several such carbidic transition metal surfaces are known to be similarly active but although some photoemission studies of such surfaces have been performed [e.g., on Ni{111} (Ref. 2) and Ni{110} (Ref. 3)] the only previous detailed band mapping study of a carbon overlayer by ARUPS appears to be the study of the catalytically *inactive* graphitic phase on Ru(0001) (Ref 4).

The particular case of the Ni{100}(2×2)C structure is of special interest, however, because the chemisorbed carbon in this structure is known to induce a reconstruction of the top nickel surface layer.[5] Low energy electron diffraction (LEED) patterns show characteristic beam absences which indicate the space group of this structure is $p4g$ (Ref. 6) and the associated glide lines can best be interpreted as implying a rotation of the groups of nickel atoms surrounding the fourfold hollow adsorption sites on the surface. A quantitative LEED analysis[5] indicates that the carbon atoms are situated in these hollow sites which are enlarged through the rotation and translation of the top layer nickel atoms. Figure 1(a) shows this real space structure schematically while Fig. 1(b) shows the various corresponding Brillouin zones. Note that the carbon coverage is 0.5 monolayers with the carbon atoms defining a $c(2\times2)$ mesh. However, the true mesh is (2×2) due to the opposite rotational sense of the nickel atom displacements around the "centered" site in the (2×2) unit mesh. A recent study of the surface phonon bands for this (2×2)C structure[7] appears to confirm the LEED-derived structure of Fig. 1 and recent work also indicates that a similar (2×2)N structure may be formed,[8,9] particularly through decomposition of NH_3 over the surface. This nitrogen structure also shows $p4g$ symmetry and therefore probably involves a similar reconstruction. By contrast, oxygen adsorbed on Ni{100} to the same half-monolayer

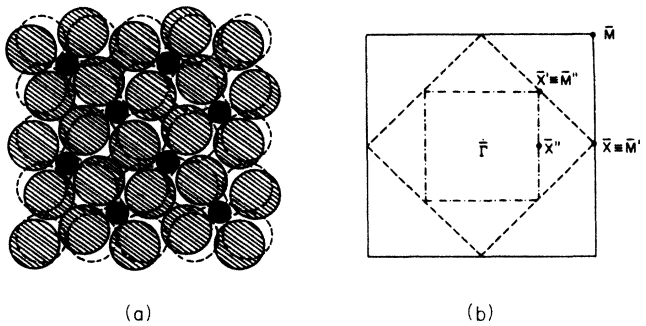

FIG. 1. (a) Schematic plan view of the proposed structure (Ref. 5) of Ni{100} (2×2)C. The small filled circles represent C atoms, the large hatched circles top layer Ni atoms. The dashed circles show the positions of the top layer Ni atoms before the reconstruction. The lateral movements of these Ni atoms are shown at their maximum hard-sphere values; structure analysis indicates the true values are not so large (Ref. 5). (b) Brillouin zones corresponding to (a). Solid lines and unprimed symmetry points indicate the (1×1) zone, dashed lines and single primed symmetry points the $c(2\times2)$ zone, and the dashed-dotted lines and double primed points the (2×2) zone.

coverage involves occupation of the same fourfold hollow sites[10] but leads to a $c(2\times2)$ structure with no reconstruction. In order to investigate this difference and to try to cast some light on the nature of the adsorbate-induced reconstruction we have carried out some comparative studies of the $c(2\times2)$O structure as well as of the (2×2)C and (1×1) clean surface structures.

In the following sections we describe briefly the experimental and theoretical methods we have used in this study. We then present the main results in the form of theoretical and experimental two-dimensional band structures for those features induced by the adsorption of carbon on Ni{100} to form the (2×2)C structure. Finally these data, and other relevant results, are discussed in the context of the reconstruction and the adsorbate-substrate and adsorbate-adsorbate interactions of the surface carbide phase.

II. EXPERIMENTAL DETAILS

The experiments were performed at the National Synchrotron Light Source at Brookhaven National Laboratory taking light from the 750-MeV storage ring using a 6-m torroidal grating monochromator and high-resolution angle-resolving electron spectrometer described in detail elsewhere.[11,12] The Ni{100} sample, prepared in the usual way, was cleaned by neon ion bombardment which removed impurities other than carbidic carbon, and by exposing the crystal at 400 °C to molecular oxygen in order to remove this remaining carbon. The oxygen left on the surface after this treatment was removed by heating to 500–550 °C. Many cycles of cleaning were needed to deplete the carbon impurity level in the subsurface region to prevent carbon segregating to the surface in this final anneal. Although we concentrate here on the spectral features associated with the (2×2)C phase, extensive clean surface measurements were made under identical incidence and take-off conditions in order that the weak carbon-induced features could be positively identified. During studies of the clean surface the sample was periodically flashed to 400 °C to remove CO adsorbed from the background (at a typical pressure of $2\text{–}4\times10^{-10}$ Torr), care being taken to check for carbon segregation to the surface during this treatment. The (2×2) carbide phase was formed by exposing the crystal at $\sim$250 °C to ethylene gas at local pressures (from a gas doser) estimated to be about 10^{-7} Torr. Both the clean surface and the (2×2)C phase were monitored by Auger spectroscopy and LEED. The (2×2)C structure showed a LEED pattern at normal incidence with the $(0,0.5n)$ and $(0.5n,0)$ beams missing (with n an odd integer), the features characteristic of the $p4g$ symmetry. The Auger electron spectrum for this phase showed the C *KVV* line shape characteristic of carbidic carbon on this surface.[1]

Photoemission experiments were conducted in two principal geometries; one with the electron spectrometer in the plane of incidence (and of polarization) of the light incident at 45° to the surface normal, and the second in the plane perpendicular to this and containing the surface normal, in this case with 25° incidence angle. By making all measurements in the ⟨110⟩ and ⟨100⟩ mirror planes of the Ni{100} substrate, photoemission selection rules[12] ensure that the first geometry samples only initial states of even parity relative to the mirror plane, while the second yields a mixture of odd and even states. Spectra showing only odd parity states can be obtained only at normal incidence and by collecting electrons in the out-of-plane geometry and this was only possible at large ($\gtrsim$40°) take-off angles due to the intrusion of the electron spectrometer in the light beam. Positive identification of odd symmetry initial states was aided, however, by additional measurements at fixed take-off angles relative to the crystal in the out-of-plane geometry and at several different incidence angles; the relative emission intensity from odd symmetry states in such an experiment is expected to grow as the incidence angle is reduced. The applications and limitations of this technique have been reviewed elsewhere.[13]

Most photoemission data were collected at photon energies of 37 and 45 eV, after tests had been made in the range 25–45 eV to establish the conditions under which the additional, carbon-induced, features could be best observed.

III. THEORETICAL DETAILS

The electronic structure of the clean and carbon covered Ni{001} surface was calculated using the self-consistent Full-potential linearized augmented-plane-wave (FLAPW) method.[14] This method has been shown to give very accurate solutions to the (local) spin-density functional equations.[15] The surfaces were modeled by a slab consisting of five layers of nickel plus a $c(2\times2)$ overlayer of either carbon atoms or "empty" spheres in the fourfold hollows. No shape approximations were made to either the density or potential and all nonmuffin-tin contributions to the Hamiltonian were taken into account self-consistently. In addition, the spin-polarization of the density, i.e., magnetism, was included in the calculations and will be discussed elsewhere.[16]

The carbon covered surface was approximated as a $c(2\times2)$ structure for computational reasons. The present $c(2\times2)$ calculations involve 10 Ni and 2 C atoms per unit cell; the correct $p(2\times2)$ structure doubles these numbers making the calculations unwieldy. While features that are associated with the surface reconstruction obviously cannot be obtained from this calculation, one still expects that the main carbon-induced features will be given approximately. The difference between the unreconstructed and reconstructed surfaces can be expressed in terms of a pseudopotential, which for small displacements, is also small. Differences in the electronic structure between the $c(2\times2)$ and $p4g$ structures will depend on this pseudopotential, which is much weaker than the bare C-Ni interaction. Hence, the electronic structure should be dominated by the $c(2\times2)$ net and its associated interactions and symmetries.

This discussion brings up the question of comparing the results of a ground-state calculation to experiment. The calculated eigenvalues are not directly related to the quasi-particles energies measured in experiment, but the correspondence is best for the more delocalized states for

which a band theory description is valid. Comparison between theory and experiment for Ni is particularly difficult since final-state effects are known to be important in order to describe the Ni d-band width. Bearing these difficulties in mind, however, one still expects a correspondence between the experimental and theoretical results although possibly slightly misplaced in energy.

IV. RESULTS AND DISCUSSION

The main results consist of the computed, and the experimentally determined, two-dimensional band structures. Figure 2 shows the results of the full slab calculation for a $c(2\times2)$ overlayer of C atoms on Ni{100} with the C atoms adsorbed in the fourfold hollow sites with a spacing of the C layer and the top Ni atom layer of 0.58 Å corresponding to a Ni-C nearest neighbor distance of 1.85 Å. This structure is similar to the LEED determination of the (2×2)C structure except that it fails to take account of the top Ni atom layer reconstruction. Because this reconstruction opens up the fourfold hollow sites, the interlayer spacing at a similar C-Ni nearest neighbor distance (1.80 Å) is smaller (0.1 Å) in the LEED result. Clearly the failure to include the reconstruction

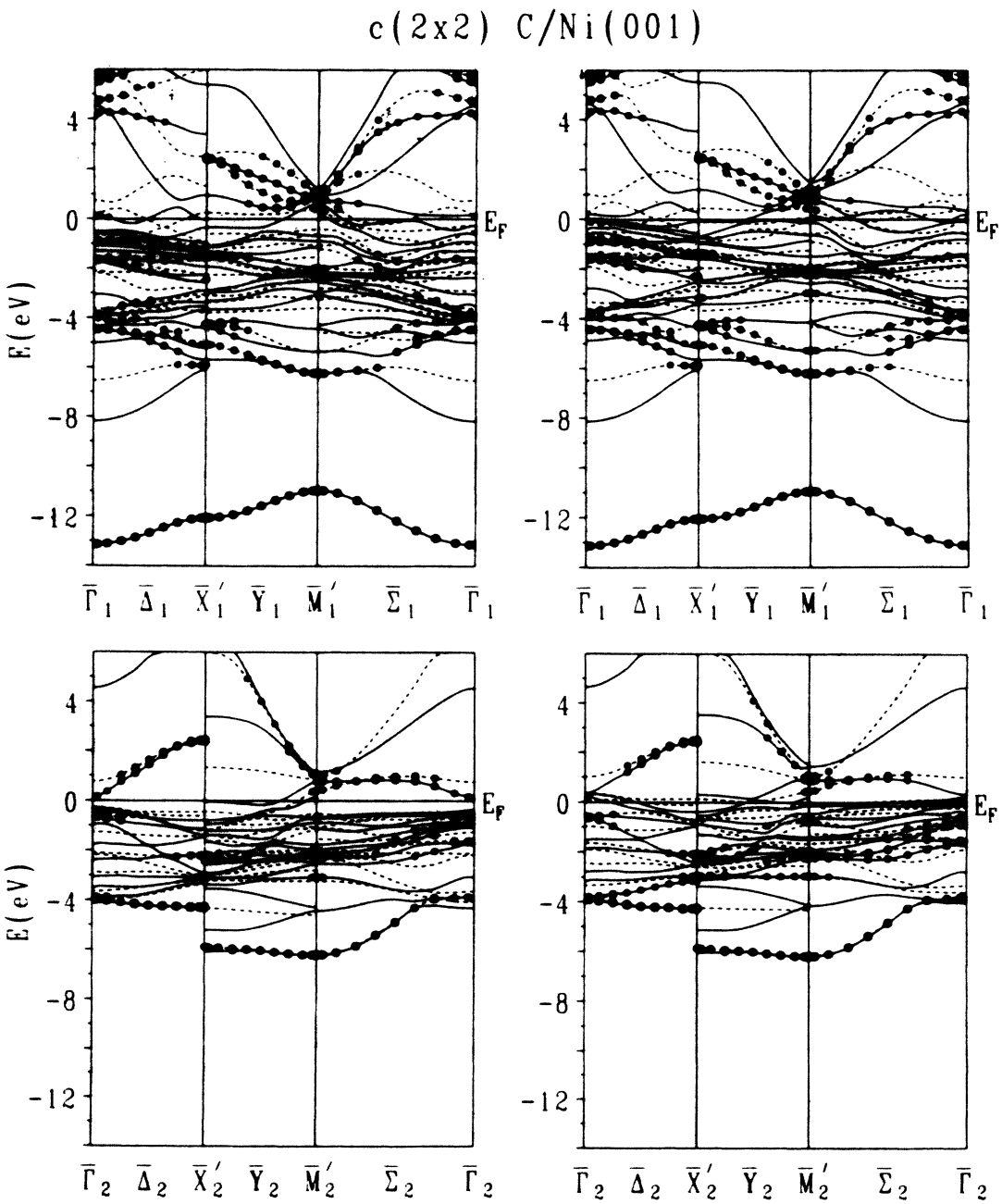

FIG. 2. Computed two-dimensional band structures for the Ni{100} $c(2\times2)$C model calculations to the even (top) and odd (bottom) parity states and for majority (left) and minority (right) spin states. Circles are plotted on those states having more than 65% weight at the surface. Note that band symmetries can change upon changing symmetry lines in the surface zone.

means that some aspects to the electronic structure will not be correctly reproduced. Unfortunately, as discussed above, the true $p(2\times2)$ structure is computationally unwieldy for this sophisticated calculation. We might have hoped that the electronic structure of the *unreconstructed* surface would give some clue to the origin of the reconstruction but there are no obvious features in the results in Fig. 2 to help us understand this effect. In order to identify those parts of the band structure which are most strongly associated with the carbon adsorption and its interaction with the surface layers of the metal, those states having more than 65% of their weight in the surface layer are marked with circles in Fig. 2. For comparison, Fig. 3 shows similar plots for the clean Ni{100} surface but with the bands folded back into the same $c(2\times2)$ first Brillouin zone. The k-space indexing in all figure is with respect to this $c(2\times2)$ zone with the symmetry points labeled as $\bar{X}'$ and $\bar{M}'$ to distinguish them from the (1×1) Ni{100} zone points $\bar{M}$ and $\bar{X}$ [with $\bar{X}\equiv\bar{M}'$ as in Fig. 1(b)].

To give some indication of the relative roles of adsorbate-adsorbate and adsorbate-substrate interactions

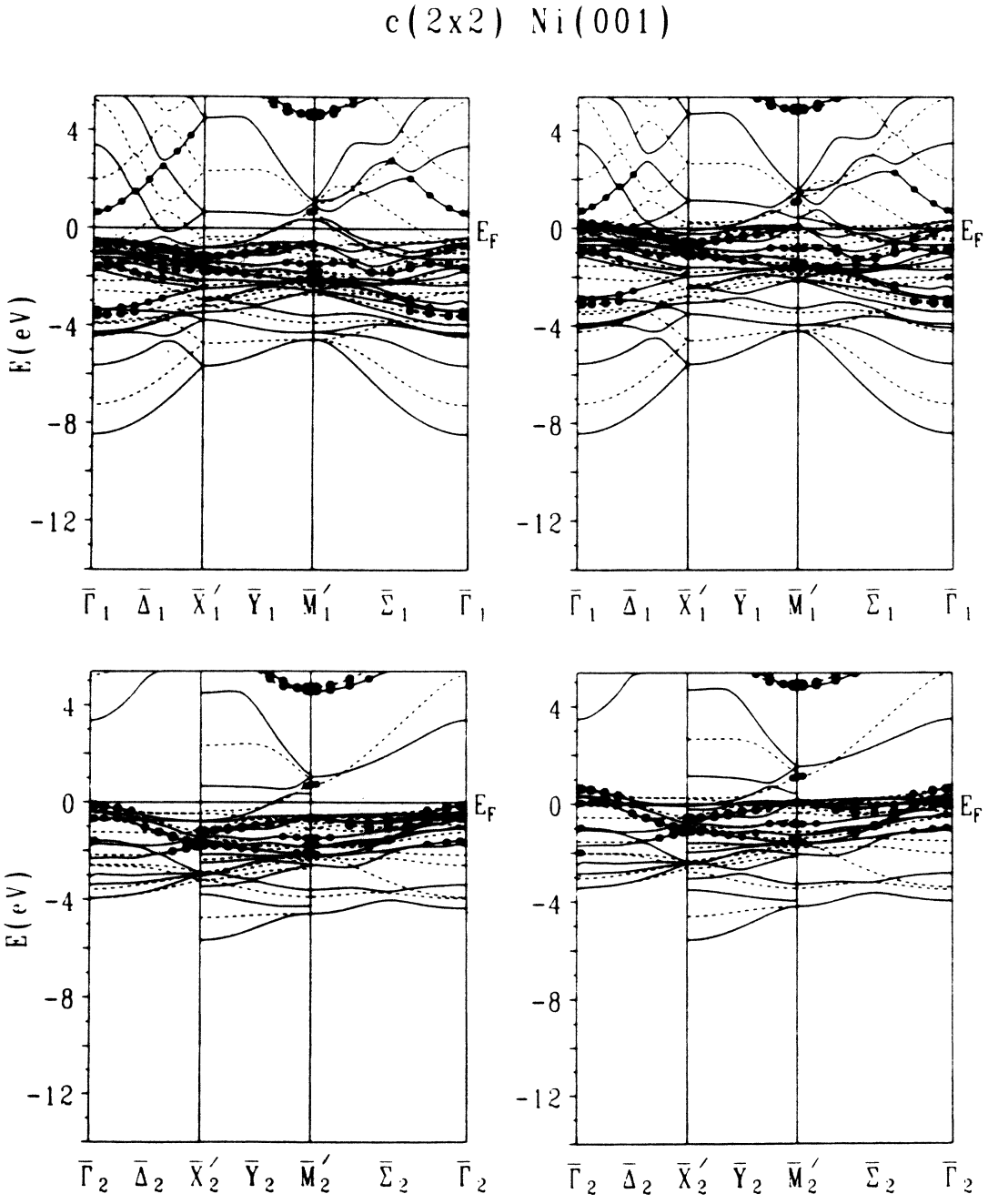

FIG. 3. Computed two-dimensional band structures for clean Ni{100} folded back into the $c(2\times2)$ surface Brillouin zone. Otherwise as Fig. 2.

in determining the band structure of Fig. 2, the results of similar calculations for a single layer of carbon atoms on the same $c(2\times2)$ lattice are shown in Fig. 4. In this case the states can be clearly labeled as derived from the C $2s$, $2p_z$, $2p_{x,y}$ states [the x and y axes being defined relative to the same $c(2\times2)$ mesh used to plot the band structure]. Comparison of Figs. 2 and 4 shows that the well-separated C $2s$ states are pulled down in energy by more than 4 eV by interaction with the nickel substrate and the dispersion is also substantially increased.

The main experimental data (measured only along $\bar{\Gamma}\bar{X}'$ and $\bar{\Gamma}\bar{M}'$ but beyond the first Brillouin zone) are presented in the same form in Fig. 5. In addition to plotting the energy-wave vector locations of carbon-induced features in the spectra, this figure shows two additional pieces of information. First, shown as shaded regions are the parts of k space in which our spectra from the clean surface show sufficiently strong features for all but the strongest adsorbate-induced features to be lost in the substrate emission. Generally the carbon-induced features in the spectra are not strong and we have taken the rather demanding view that only clearly resolved features, not seen in the equivalent clean surface spectra, should be plotted in Fig. 5. We have therefore not made use of difference spectra which, particularly for angle-resolved studies, can be potentially misleading. For this reason the shaded regions indicate sections of $\mathbf{k}$ space in which adsorbate-induced states would only be detected if they had substantial photoemission cross sections. Also shown in Fig. 5 as full lines are those bands of the full calculations (Fig. 2) with more than 75% weight in the surface region (including both majority and minority spins which cannot be distinguished in the experiment). Note that in plotting the experimental points, the circles represent photoemission peaks which correspond to $\mathbf{k}_{||}$ values in the first $c(2\times2)$ Brillouin zone while squares relate to peaks seen in higher zones and folded back into the first zone.

In some cases the carbon-induced features were very weak in the first $c(2\times2)$ Brillouin zone but appeared strongly in higher zones. Figure 6 shows a typical set of

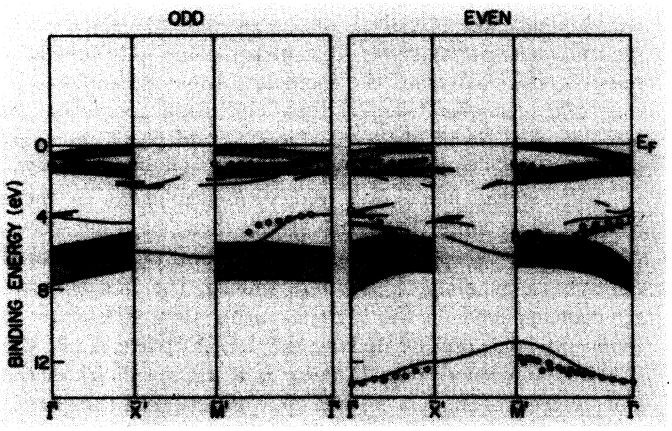

FIG. 5. Comparison of experimentally derived two-dimensional band-structure data points for the (2×2)C structure with the results of the theoretical calculations. Theoretically computed bands, of both spins, having more than 75% weight on the surface are shown as full lines. The shaded regions indicate where experimental photoemission peaks occur from the clean Ni{100} surface. Circles represent $k_{||}$ values in the first zone while squares relate to measurements folded back from higher zones.

photoemission spectra which illustrate this effect. At normal emission only the shoulder near 4.0-eV binding energy is due to carbon, while strong features only appear at emission angles greater than about 30°. Note, in particular, the C $2p$—related peak around 4—6 eV binding energy and a peak within the d band at a binding energy of about 1 eV. $\bar{M}$, which folds back to $\bar{\Gamma}$ in the $c(2\times2)$ structure, is sampled at about 40° emission angle at this photon energy (37 eV).

One final remark regarding the experimental data points in Fig. 5 concerns the distinction between odd and even parity states, particularly in the $\bar{\Gamma}\bar{M}'$ direction. As

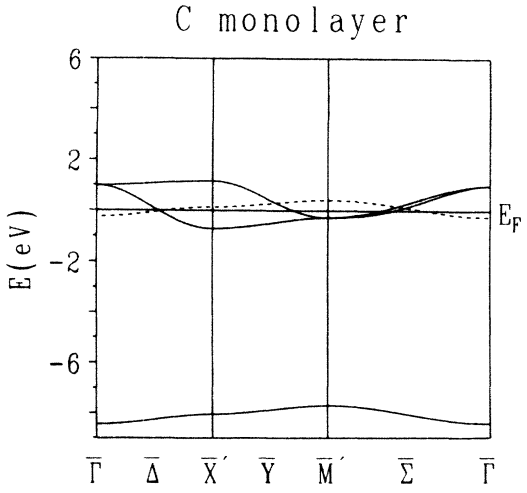

FIG. 4. Computed two-dimensional band structure for an isolated $c(2\times2)$C layer. The p_z band is dashed.

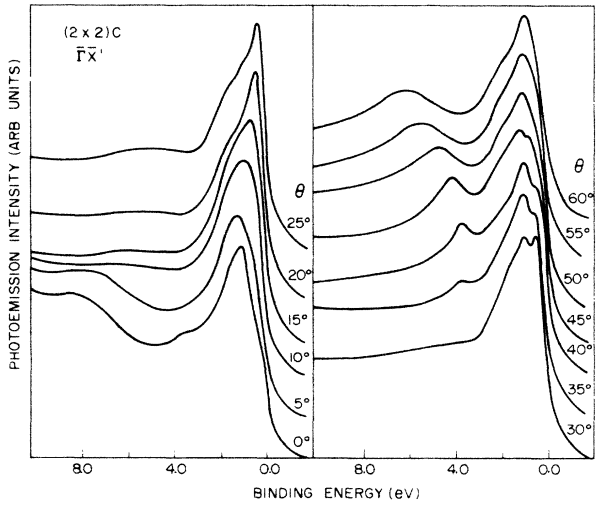

FIG. 6. Photoemission energy distribution spectra recorded at various angles of emission in the $\bar{\Gamma}\bar{X}'$ azimuth for a photon energy of 37 eV from the Ni{100}(2×2) structure.

we have already described, our measurements will clearly identify even parity states in a mirror plane but odd states must be inferred from the incidence angle dependence in the "odd plus even" out-of-plane collection geometry. In fact (see Fig. 5) all observed states of odd parity lie energetically close to states of even parity. However, the intensities of the associated photoemission peaks in these cases behave quite differently from those of other states which have even parity alone. The second point concerns the symmetry along $\bar{\Gamma}\bar{M}'$ and, indeed, the fact that we are plotting data on the $c(2\times2)$ rather than true $p(2\times2)$ Brillouin zone represented by the LEED pattern. In the (2×2)C structure (Fig. 1) there is a mirror plane in the $\bar{\Gamma}\bar{X}'$ direction [which is the $\bar{\Gamma}\bar{M}''$ direction of the (2×2) mesh] but along $\bar{\Gamma}\bar{M}'$ ($\bar{\Gamma}\bar{X}$) there is only glide line symmetry. This reduced symmetry derives only from the reconstructed top layer Ni atoms, the substrate and carbon overlayer retaining the mirror plane. This same reconstructed layer is the only element of the structure reducing the size of the reciprocal net from $c(2\times2)$ to $p(2\times2)$. In fact the experimental data indicate that the electronic structure is dominated by the $c(2\times2)$ net and its associated symmetry. Thus the mirror plane selection rules appear to distinguish states satisfactorily along $\bar{\Gamma}\bar{M}'$ while the C $2s$ related peak around 12–13 eV binding energy clearly folds back at the $\bar{M}'$ point of the $c(2\times2)$ mesh and not halfway along $\bar{\Gamma}\bar{M}'$ at $\bar{X}''$. In this sense, therefore, the experimental data are clearly best compared with calculations for the $c(2\times2)$ mesh structure although the LEED patterns clearly show the (2×2) reconstruction. In fact, observations of surface-related states dispersing according to a larger unit mesh than that seen in LEED are by no means rare.[17]

In many respects the agreement between theory and experiment displayed in Fig. 5 is very satisfactory. At $\bar{\Gamma}$ the energies of both the C $2s$ and C $2p$ related states around 13 and 4 eV binding energy are reproduced well; in view of the marked contribution of the adsorbate-substrate interaction indicated by comparison of Figs. 2 and 4 this is a significant result. The degree of dispersion in both regions, however, is probably overestimated by the calculations although in the C $2s$ band it is clear that the experimentally observed dispersion is greater than that predicted for the isolated carbon layer, indicating that adsorbate-substrate as well as adsorbate-adsorbate interactions are important in establishing the dispersion of this band as well as it energetic location. Theory and experiment are also in agreement over the dominant dispersion direction (to deeper binding energies away from $\bar{\Gamma}$) for the observed C $2p$-related states around 4–5 eV binding energy. Some features below the Ni d band predicted by the theory are not observed experimentally although this may, of course, be due to low photoemission cross sections. In particular, no state is seen near 4 eV binding energy of odd parity ($2p_y$-derived) in the $\bar{\Gamma}\bar{X}'$ direction while the bottom of the odd symmetry $2p$-related state near $\bar{M}'$ is not seen. As may be seen from comparison of Figs. 2 and 3, this state lies below the calculated Ni bands and so might be expected to be easily observed. In fact substrate emission *is* seen in this energy range, probably deriving contributions from both even parity state emission and from the many-body excitation observed in this region of the photoemission spectrum from nickel.[18]

Although this agreement for the lower-lying states is extremely encouraging, features relevant to the reconstruction might be expected to be found closer to the Fermi level. For example, one view of the driving force for some clean metal surface reconstructions is that if a surface state of the unreconstructed surface crosses the Fermi level midzone, the band gap opened by the reconstruction could result in a reduction of the total energy. This, and other arguments also relating to the Tamm surface states separated from the d band close to the Fermi level have been proposed, for example, to understand the reconstruction of W{100} (Ref. 19). [It should be noted that this interpretation has been questioned[19] even for W(001).] In the case of Ni{100} the only surface states proposed appear to be spin-specific ("magnetic") ones close to $\bar{X}$ and $\bar{M}$ (Ref. 20). In addition to the possible role of states close to the Fermi level in influencing the reconstruction, Feibelman has proposed that a key feature of the catalytic activity of the carbided Ru(0001) surface is the presence of C $2p_z$–derived states close to the Fermi level.[21]

As may be seen in Fig. 5, we do, in fact, observe experimentally a clear carbon-induced state over much of the surface Brillouin zone in the nickel d band, with a binding energy around 1.0 eV. Moreover, comparison of the photoemission data with those from the clean surface reveals a clean surface feature just below the Fermi level, particularly around midway along $\bar{\Gamma}\bar{M}'$ which is strongly suppressed by carbon adsorption. By contrast, measurement on the $c(2\times2)$O structure on Ni{001}, in which the oxygen occupies the same fourfold hollow sites but does not cause substrate reconstruction, show neither strong suppression of the substrate feature nor development of the extra d-band peak. These effects are seen in the representative spectra shown in Fig. 7, taken at 37 eV photon energy and take-off angles of 12.5° and 22.5° along $\bar{\Gamma}\bar{M}'$ corresponding $k_{||}$ values for states close to the Fermi level of approximately 0.62 and 1.10 Å^{-1} ($\bar{M}'$ is at 1.26 Å^{-1}). These effects are not obviously predicted by the computed band structures of Figs. 2 and 3. While for the clean surface, minority states of both even and odd symmetry exist near the Fermi level near $\bar{M}'$, these states, although surface enhanced, are not particularly localized to the surface. (The states of interest have only on the order of 50% of their weight at the surface). Likewise, the $c(2\times2)$C calculations do not show any highly localized features that are obviously carbon induced in this energy range. Hence the calculations do not support a Fermi surface nesting-type driving force for the reconstruction, but suggest rather a local bonding or electrostatic origin.

Extracting more detailed information from the computed band structure of Fig. 2 in the d-band region is difficult, however, because of the many bands which are present. Some further information can be gained by plotting the computed densities of states at specific atomic sites. Figure 8 shows a pair of these, evaluated at top layer Ni atom sites (which are adjacent to C atoms in the adsorption structure) for the minority spin states. The density of d states is generally much higher than of s and p states which are barely visible on the same scale. At deeper

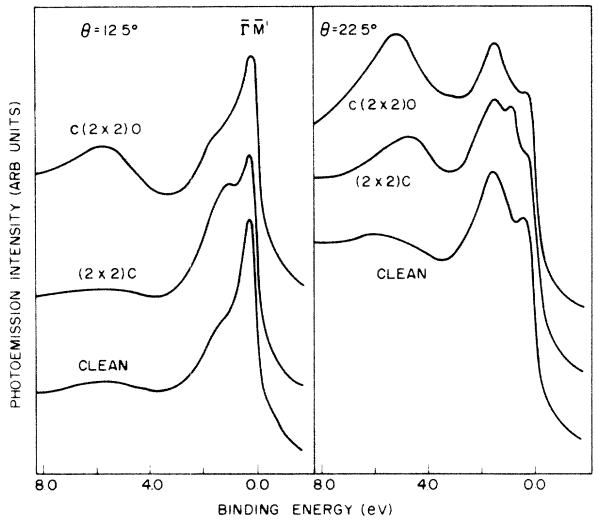

FIG. 7. Comparison of photoemission spectra at two takeoff angles in the $\bar{\Gamma}\bar{M}'$ azimuth at a photon energy of 37 eV for clean Ni{100}, the (2×2)C overlayer, and a $c(2\times2)$O overlayer.

binding energies significant extra density of states, at the metal atoms, is seen in the C $2p$ and C $2s$ regions. At the Fermi level there is a strong suppression of the metal (minority spin) d states. Plots of the majority spin states are qualitatively similar although in this case there are no states at (or above) E_F to suppress. Evidently this difference between the majority and minority spin states leads to a strong loss of magnetic moment in the surface layer following carbon adsorption. Of particular interest in comparison with experiment is that the density of states plots do provide some basis for understanding the loss of photoemission intensity close to E_F on carbon adsorption, but do not show any obvious feature which can be correlated with the additional intensity at a binding energy of about 1.0 eV.

In view of the absence of this feature from the theoretical results or from the oxygen adsorption structure it is tempting to ascribe it to the reconstruction; we note that the role of carbon $2p_z$-related states of the kind discussed by Feibelman is already included in the calculation which fails to predict the new peak. Although the suppression of the photoemission intensity close to E_F can be associated with the interaction of C with the top Ni layer, it is still possible that the reconstruction may cause the d-band

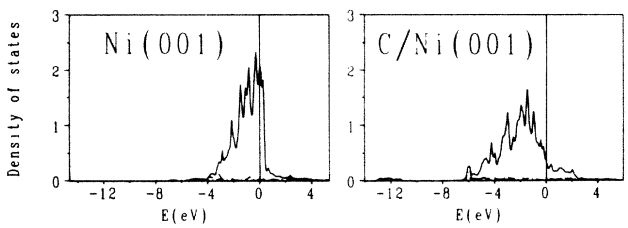

FIG. 8. Local densities of minority spin states at top layer Ni atoms calculated for the clean Ni{100} surface and the Ni{100}$c(2\times2)$C surface in states/eV.

structure of this single Ni layer to be modified significantly. In particular, if the d-band states were shifted down in energy for this layer we might observe qualitative changes of the kind seen in Fig. 7. The loss of photoemission intensity close to the Fermi level and the new peak at somewhat lower energy could therefore be correlated and characteristic of the top layer reconstruction. Presumably this energy lowering of the d band for the reconstructed layer could also be related to the overall reduction of energy which must occur if the structural change is to be favored. Furthermore, we note that since the minority density of states at the Fermi level is strongly suppressed, such a shift of the d bands is possible without drastically upsetting the approximate layer-by-layer charge neutrality, and hence without incurring the large energy penalty associated with charging of the surface. Of course, this separation of the features into metal d band and C $2p$ is somewhat artificial in that the reconstruction does not occur on the clean surface, but only on interaction with the adsorbed carbon layer. Nevertheless, these d-band features may well be the fingerprint of the electronic structure changes which characterize the positional rearrangement.

V. CONCLUSION

Comparisons of ARUPS data from the Ni{100} (2×2)C structure with slab calculations for this system which fail to include the top layer reconstruction of the real surface show good agreement in the energetic location of the carbon-induced features below the Ni d band. In particular the energies at $\bar{\Gamma}$ of the C $2s$- and C $2p$-derived features are in excellent agreement and while the qualitative character of the dispersion of these states is also reproduced in the calculations, the absolute magnitude of these dispersions appears to be somewhat overestimated. The C $2s$ states, for example, show a bandwidth midway between that calculated for an isolated carbon layer and for the same layer interacting with the Ni substrate. Both the energy location and dispersion of these states is very different to those found for graphite overlayers on Ni{100} (Ref. 22). In addition the experiments reveal changes in the d-band region close to the Fermi level which are not seen in either the calculations or in experiments on the $c(2\times2)$O structure. We propose that these changes are characteristic of the carbon-induced reconstruction of the top substrate layer. In view of the fact that recent work indicates a similar reconstruction can be induced by the adsorption of nitrogen, an ARUPS study of this system would also be of considerable interest.

ACKNOWLEDGMENTS

This research was carried out in part at the National Synchrotron Light Source (NSLS), Brookhaven National Laboratory, which is supported by the U.S. Department of Energy (Division of Materials Sciences and Division of Chemical Sciences). CFM and DPW also acknowledge the financial support of the Science and Engineering Research Council (United Kingdom).

*Present address: Department of Physics, University of Oregon, Eugene, OR 97403.

[1]R. D. Kelley and D. W. Goodman, in *The Chemical Physics of Solid Surfaces and Heterogeneous Catalysis,* edited by D. A. King and D. P. Woodruff (Elsevier, Amsterdam, 1982), Vol. 4, p. 453.

[2]R. Rosei, S. Modesti, F. Sette, C. Quaresima, A Savoia, and P. Perfetti, Solid State Commun. **46**, 871 (1983); Phys. Rev. B **29**, 3416 (1984).

[3]G. Paolucci, R. Rosei, K. C. Prince, and A. M. Bradshaw, Appl. Surf. Sci. **22/23**, 582 (1985).

[4]F. J. Himpsel, K. Christmann, P. Heimann, D. E. Eastman, and P. J. Feibelman, Surf. Sci. **115**, L159 (1982).

[5]J. H. Onuferko, D. P. Woodruff, and B. W. Holland, Surf. Sci. **87**, 357 (1979).

[6]B. W. Holland and D. P. Woodruff, Surf. Sci. **36**, 488 (1973).

[7]T. S. Rahman and H. Ibach, Phys. Rev. Lett. **54**, 1933 (1985).

[8]H. Ibach (private communication).

[9]Other indications that a Ni{100} (2×2)N structure exists may be found in R.-S. Li and L.-X. Tu, Surf. Sci. **92**, L71 (1980), and in M. Grunze, P. A. Dowben, and C. R. Brundle, Surf. Sci. **128**, 311 (1983).

[10]J. E. Demuth, D. W. Jepsen, and P. M. Marcus, Phys. Rev. Lett. **31**, 540 (1973).

[11]P. Thiry, P. A. Bennett, S. D. Kevan, W. A. Royer, E. E. Chaban, J. E. Rowe, and N. V. Smith, Nucl. Instrum. Methods **222**, 85 (1984); S. D. Kevan, Rev. Sci. Instrum. **54**, 1441 (1983).

[12]R. J. Smith, J. Anderson, and G. J. Lapeyre, Phys. Rev. Lett. **37**, 1081 (1976).

[13]E. W. Plummer and W. Eberhardt, *Advances in Chemical Physics,* edited by I. Prigogine and S. I. Rice (Wiley, New York, 1982), Vol. 49.

[14]E. Wimmer, H. Krakauer, M. Weinert, and A. J. Freeman, Phys. Rev. B **24**, 864 (1981); M. Weinert, J. Math. Phys. **22**, 2433 (1981).

[15]W. Kohn and L. J. Sham, Phys. Rev. B **140**, A1133 (1965); V. von Barth and L. Hedin, J. Phys. C **5**, 1629 (1972).

[16]M. Weinert and J. W. Davenport (unpublished).

[17]See, for example, the report of dispersion following the (1×1) surface Brillouin zone for the Si{111} ($\sqrt{3}\times\sqrt{3}$) Al structure by R. I. G. Uhrberg, G. V. Hansson, J. M. Nicholls, P. E. S. Persson, and S. A. Flodström, Phys. Rev. B **31**, 3805 (1985).

[18]C. Guillot, Y. Ballu, J. Paigne, J. Lecante, K. P. Jain, P. Thiry, R. Pinchaux, Y. Petroff, and L. M. Falicov, Phys. Rev. Lett. **39**, 1632 (1977).

[19]See, for example, J. E. Inglesfield and B. W. Holland, in *The Chemical Physics of Solid Surfaces and Heterogeneous Catalysis,* edited by D. A. King and D. P. Woodruff (Elsevier, Amsterdam, 1981), Vol. 1, p. 355; D. A. King, Phys. Scr. **T4**, 34 (1983).

[20]E. W. Plummer and W. Eberhardt, Phys. Rev. B **20**, 1444 (1979).

[21]P. J. Feibelman, Surf. Sci. **103**, L149 (1981).

[22]C. F. McConville, D. P. Woodruff, and S. D. Kevan (unpublished).

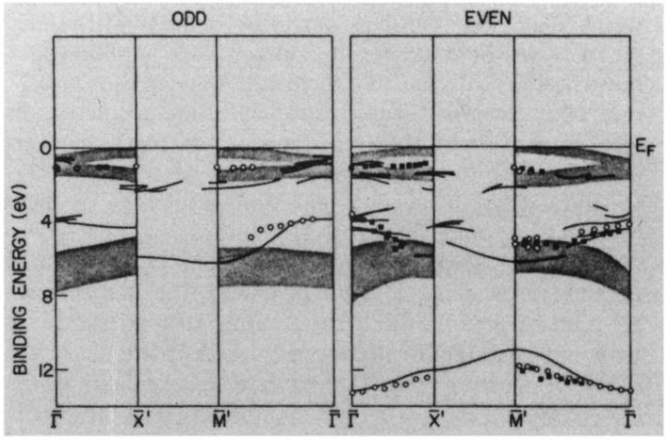

FIG. 5. Comparison of experimentally derived two-dimensional band-structure data points for the (2×2)C structure with the results of the theoretical calculations. Theoretically computed bands, of both spins, having more than 75% weight on the surface are shown as full lines. The shaded regions indicate where experimental photoemission peaks occur from the clean Ni{100} surface. Circles represent $k_{||}$ values in the first zone while squares relate to measurements folded back from higher zones.